Basilico, Hultberg et al.

Four individually druggable Met hotspots mediate HGF-driven tumor progression

Online Supplementary Material

Includes:

Supplementary Figures 1-17

Supplementary Tables 1-4

Supplementary Methods

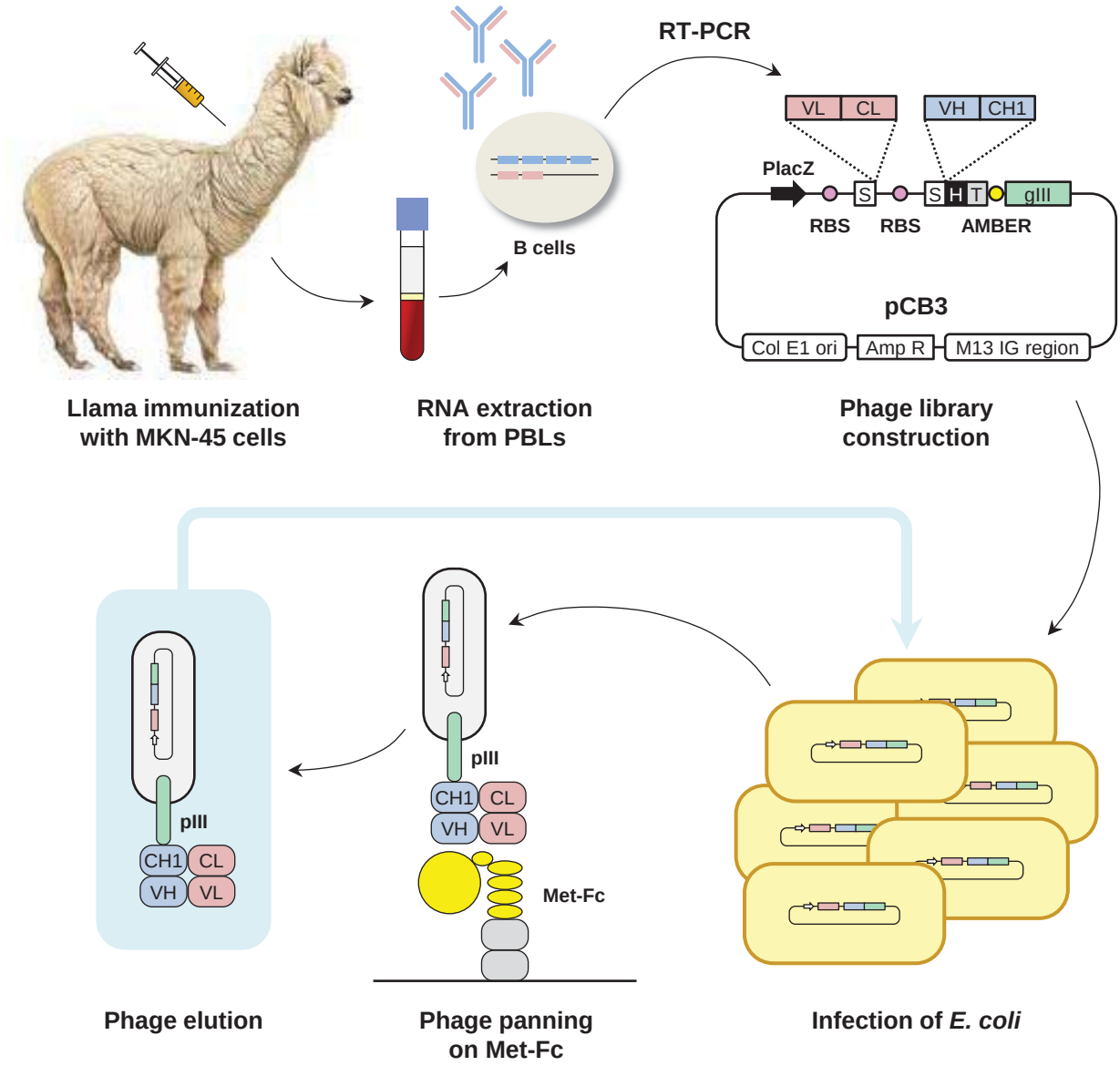

Suppl. Fig. 1. Generation of anti-human Met antibodies using a llama-based platform. Six llamas (*Lama glama*) were immunized by intramuscular injection of $1 \cdot 10^7$ MKN-45 human gastric carcinoma cells and boosted weekly with the same cell number. Seven weeks post immunization, total RNA was extracted from peripheral blood lymphocytes (PBLs), and the cDNAs encoding the VH-CH1 and VL-CL domains were amplified by RT-PCR. PCR products were subcloned into the phagemid vector pCB3 that allows expression of recombinant antibodies as Fab fragments fused to the phage pIII coat protein. Recombinant phages were panned on an immobilized chimera consisting of the Met extracellular domain fused to the Fc portion of human IgG1 (Met-Fc). Two to four rounds of affinity selections were performed to enrich the libraries for phages displaying Met-specific Fabs. PlacZ, *E. coli* lac Z promoter; RBS, ribosome binding site; S, signal peptide; H, poly-histidine; T, MYC-tag; AMBER, amber stop codon; gIII, phage gene encoding the coat pIII protein.

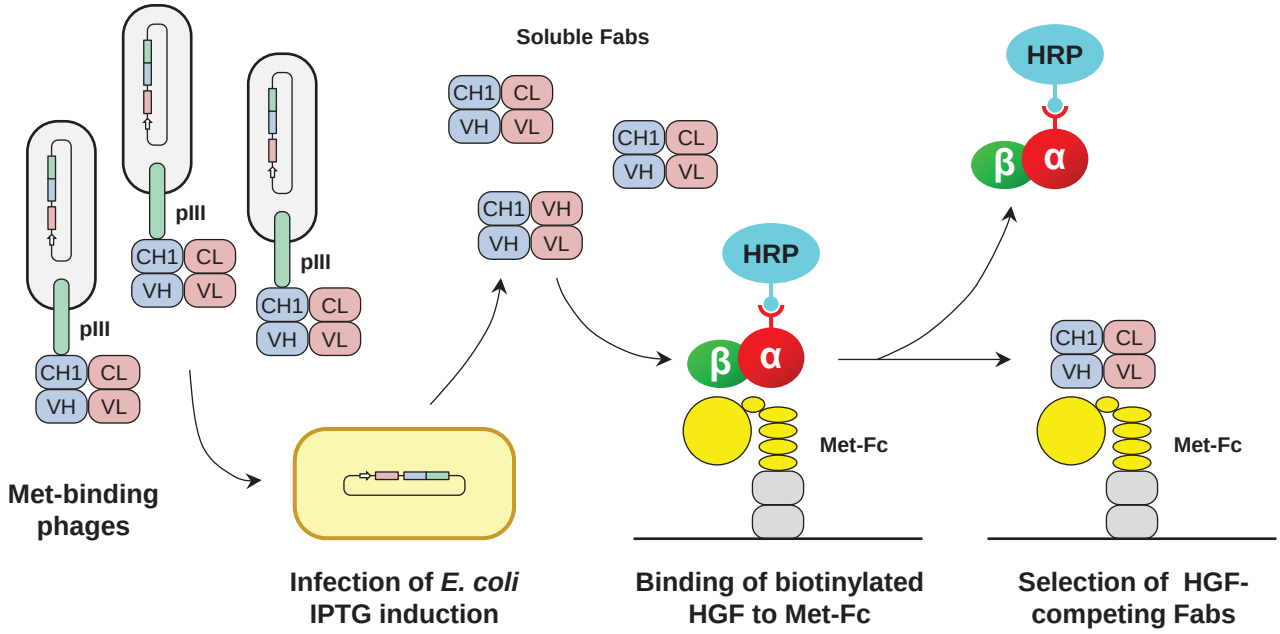

Suppl. Fig. 2. Screening of individual Fabs for their ability to compete with HGF binding to Met. Starting from the Met-binding phages identified by the panning procedure described in Suppl. Fig. 1, we induced secretion of soluble Fab fragments using IPTG. The Fab-containing periplasmic fraction of each individual clone was directly analyzed for its ability to inhibit binding of biotinylated HGF to a Met-Fc fusion protein in an ELISA assay. The pIII coat protein (in green) is the product of the gIII phage gene. HGF was biotinylated with a N-terminus-specific reaction resulting in one biotin molecule per α/β hetero-dimeric HGF molecule. Binding was revealed using streptavidin-conjugated horseradish peroxidase (HRP).

A

Clone	Library	VH family	k_{off} (10^{-4} s^{-1})
WT3	λ2	14	69
WT4	λ2	15	9
WT5	λ2	16	36
WT14	λ3	6	1.3
WT15	λ3	6	1.4
WT25	λ4	7	6.5
WT26	λ4	8	1.5
WT37	λ5	33	16
WT38	κ5	28	23
WT46	κ5	28	12
WT52	λ7	29	6.4
WT53	λ7	29	8.5
WT60	κ7	27	13

B

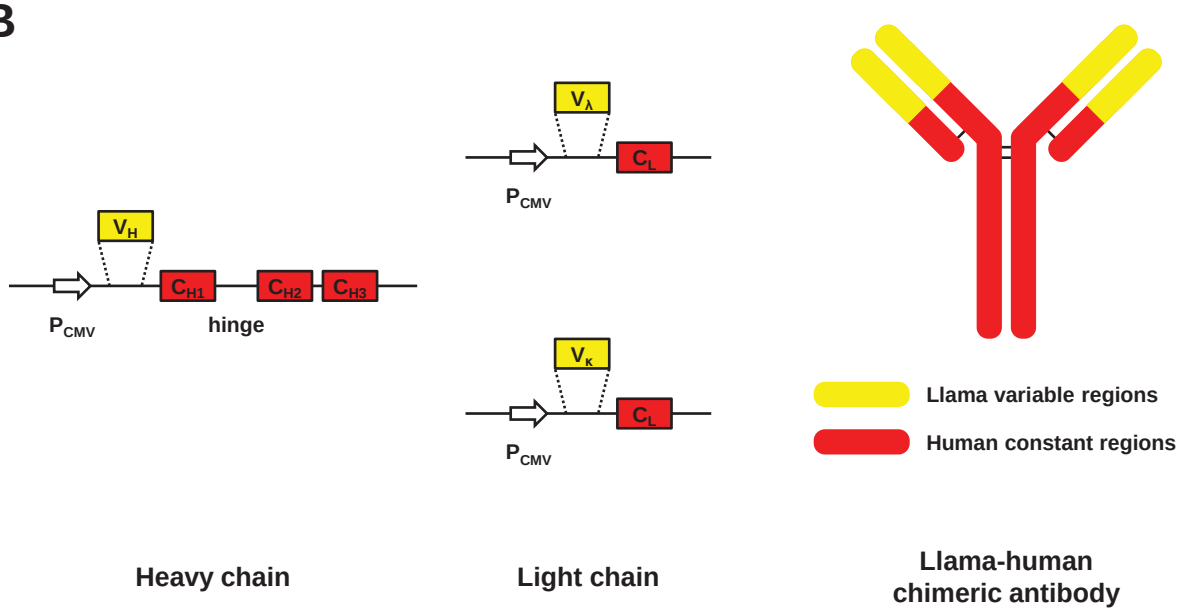

Suppl. Fig. 3. Generation of chimeric human immunoglobulins bearing llama variable regions. (A) Fabs that competed with HGF binding to Met in ELISA were analyzed by Surface Plasmon Resonance (SPR) using recombinant Met extracellular domain (Met ECD) in solid phase and Fab-containing periplasmic *E. coli* extract in soluble phase. Thirteen Fab clones displaying low off-rates (k_{off}) were selected for further analysis. (B) The VH and VL regions of the Fabs described in A were fused to human constant H domains (from IgG1) and a human constant L domain (λ or κ), respectively, to generate chimeric llama-human bivalent, monoclonal immunoglobulins. Two separate mammalian expression vectors were engineered for antibody heavy chains and light chains (either λ- or κ- type). P_{CMV}, cytomegalovirus promoter.

A

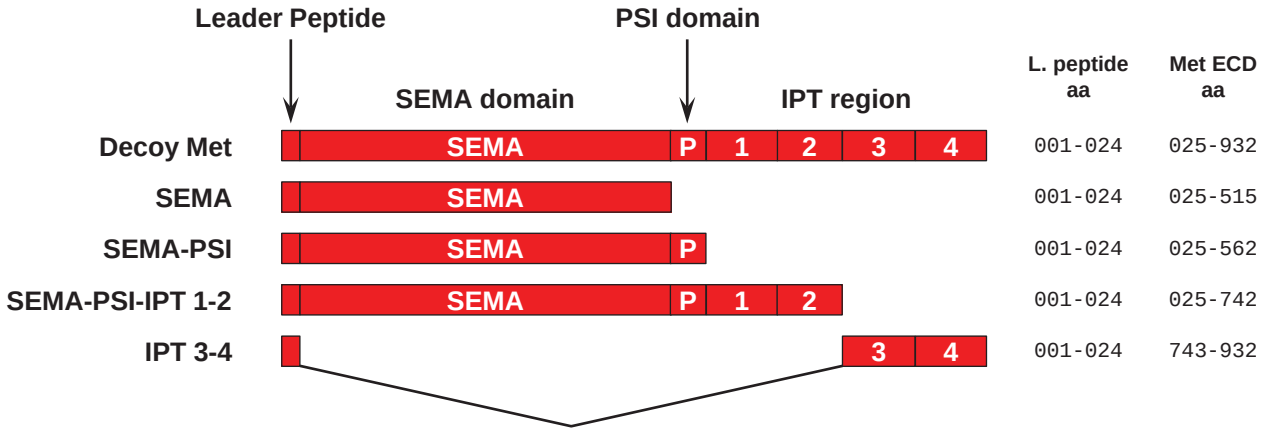

B

mAb	DM	SP12	SP	S	I34	binding domain
WT3	+	+	+	+	–	SEMA
WT4	+	–	–	–	–	IPT 2-3 ?
WT5	+	+	+	+	–	SEMA
WT14	+	+	–	–	–	IPT 1-2
WT15	+	+	–	–	–	IPT 1-2
WT25	+	–	–	–	–	IPT 2-3 ?
WT26	+	–	–	–	–	IPT 2-3 ?
WT37	+	+	+	+	–	SEMA
WT38	+	+	–	–	–	IPT 1-2
WT46	+	+	–	–	–	IPT 1-2
WT52	+	+	+	+	–	SEMA
WT53	+	+	+	+	–	SEMA
WT60	+	+	–	–	–	IPT 1-2
5D5	+	+	+	+	–	SEMA
224G11	+	+	–	–	–	IPT 1-2

Suppl. Fig. 4. HGF-displacing anti-Met mAbs recognize epitopes located throughout the extra-cellular domain of Met. (A) Engineered human Met proteins used for determining the domains of Met responsible for antibody binding. ECD, extra-cellular domain; aa, amino acid; L. peptide, leader peptide; SEMA, semaphorin homology domain; PSI or P, plexin-semaphorin-integrin homology domain; IPT 1-4, Immuno-globulin-transcription factor-plexin homology domain 1-4. (B) Binding of the various HGF-displacing mAbs to the engineered Met proteins described in A as determined by ELISA. DM, Decoy Met; SP12, SEMA-PSI-IPT 1-2; SP, SEMA-PSI; S, SEMA; I34, IPT 3-4. Color code is relative to binding domain (SEMA, orange; IPT 1-2, turquoise; IPT 2-3, green).

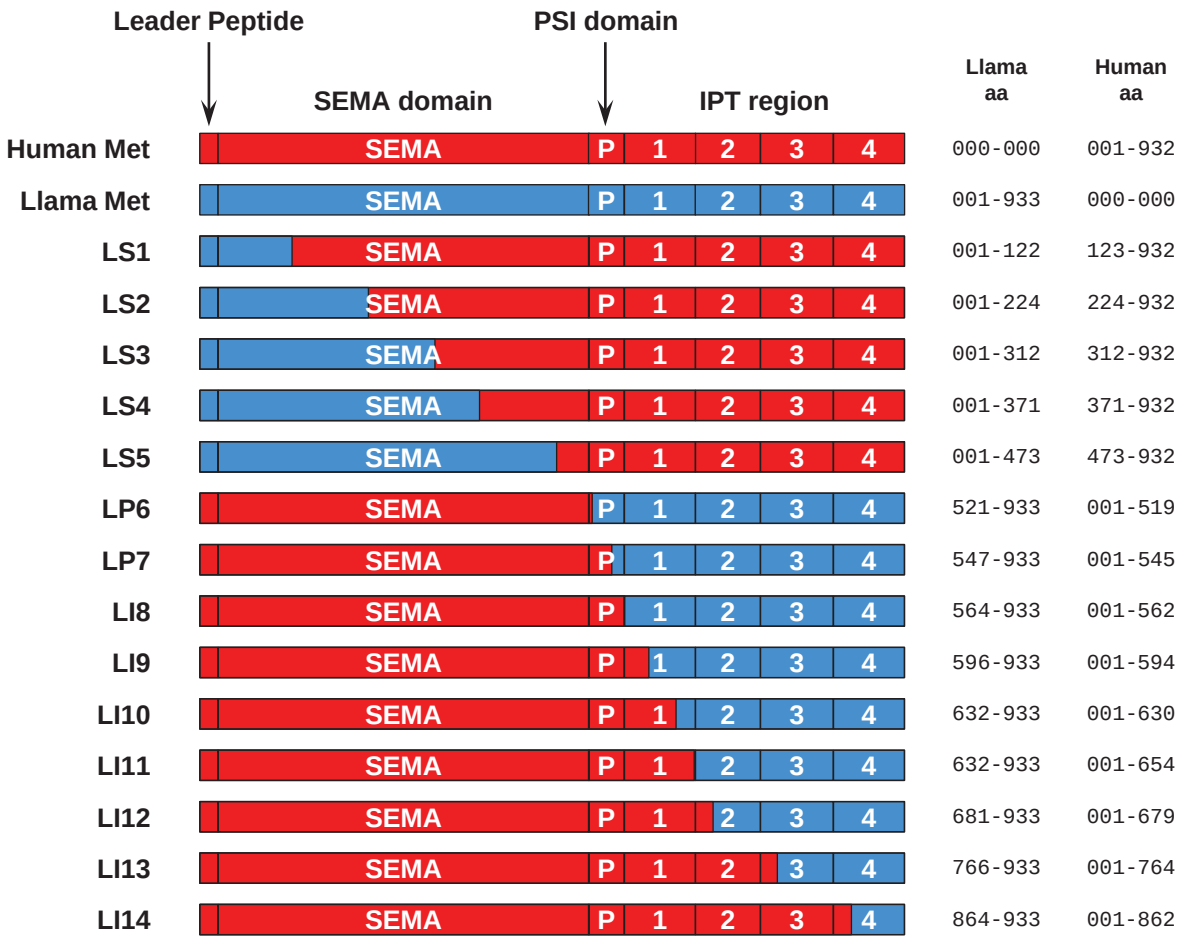

Suppl. Fig. 5. Llama-human chimeric Met proteins used for finely mapping the epitopes recognized by anti-Met antibodies. The extracellular portions of llama Met and human Met are composed of 933 and 932 amino acids (aa), respectively (llama Met contains an insertion after aa 166). Both receptor ectodomains comprise a leader peptide, a semaphorin homology domain (SEMA), a plexin-semaphorin-integrin homology domain (PSI or P) and four immuno-globulin-transcription factor-plexin homology domains (IPT). Chimeras LS1-5 have an N-terminal llama portion followed by a C-terminal human portion. Chimeras LP6-7 and LI1-14 have an N-terminal human portion followed by a C-terminal llama portion.

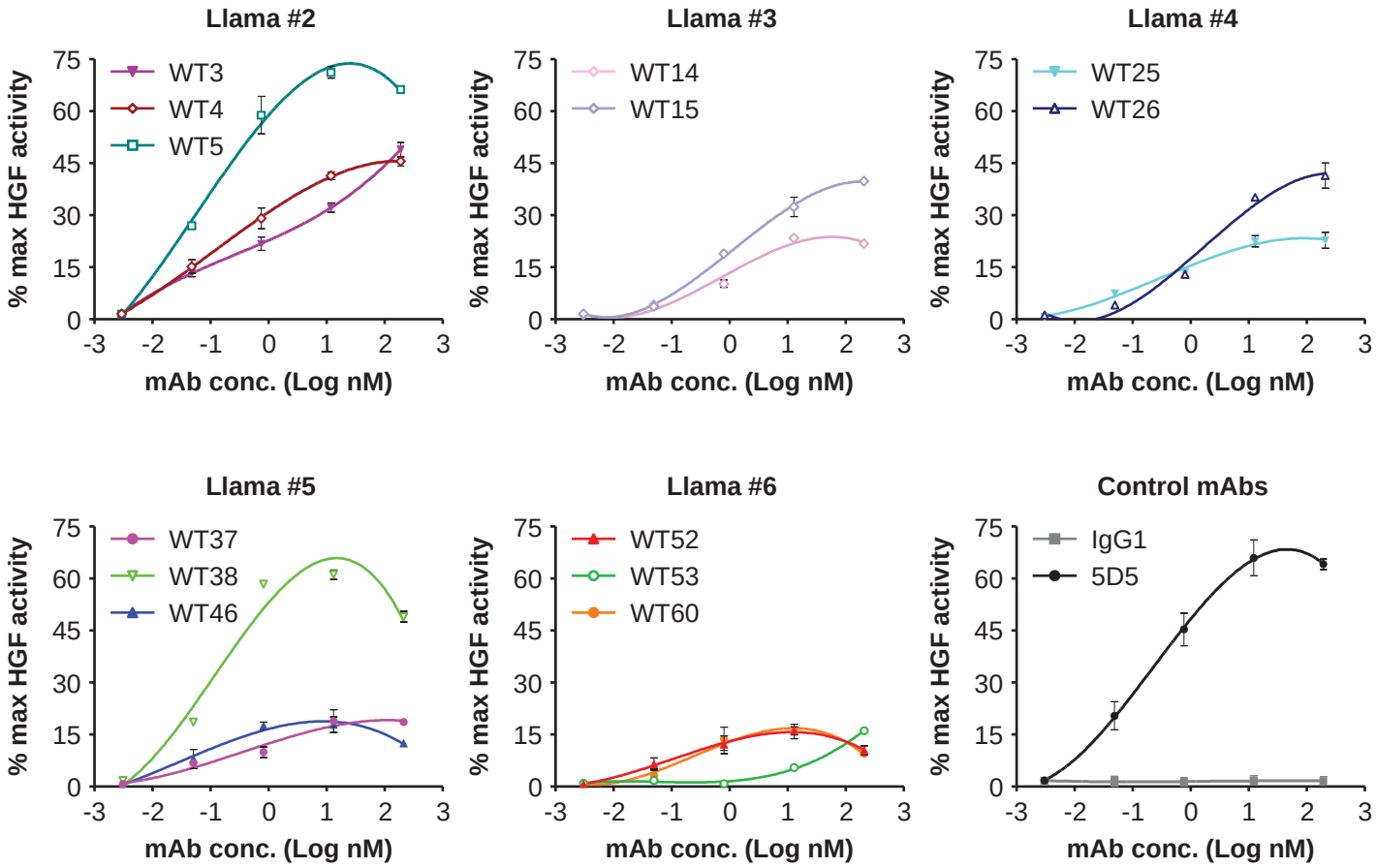

Suppl. Fig. 6. Agonistic activity of anti-Met antibodies as measured by their ability to promote Met autophosphorylation. A549 cells were stimulated with increasing concentrations (0-200 nM) of antibodies in the absence of HGF. The 5D5 antibody and an irrelevant IgG1 were used as positive and negative control, respectively. Met autophosphorylation was determined by ELISA using phospho-Met-specific antibodies. At the same time, we also stimulated cells with increasing concentrations of recombinant HGF, and determined that Met activation reached its maximum at 1 nM HGF. The agonistic activity of antibodies was expressed as percent of maximal HGF activity. Data relative to antibodies generated by different llamas are shown in separate graphs. Some experimental variability was observed in this assay. Data shown in this figure are derived from a representative experiment. The range of variation is shown in Tab. 1.

A

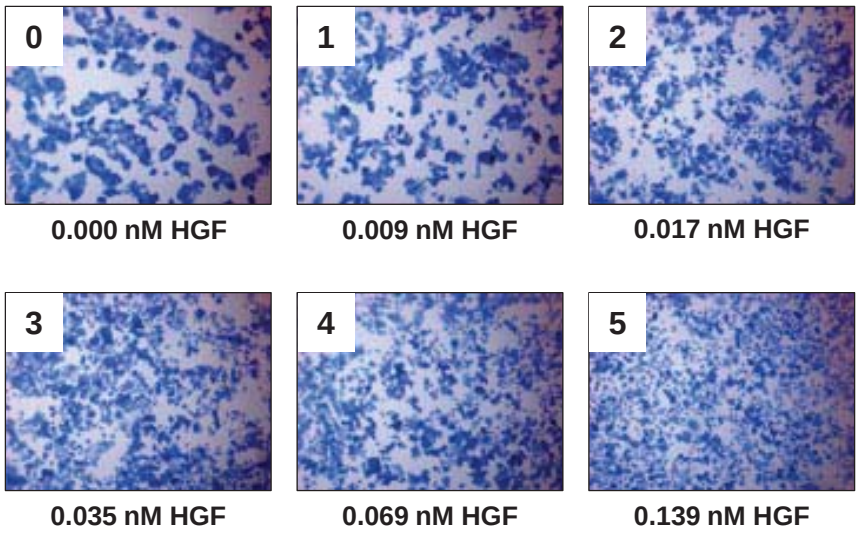

B

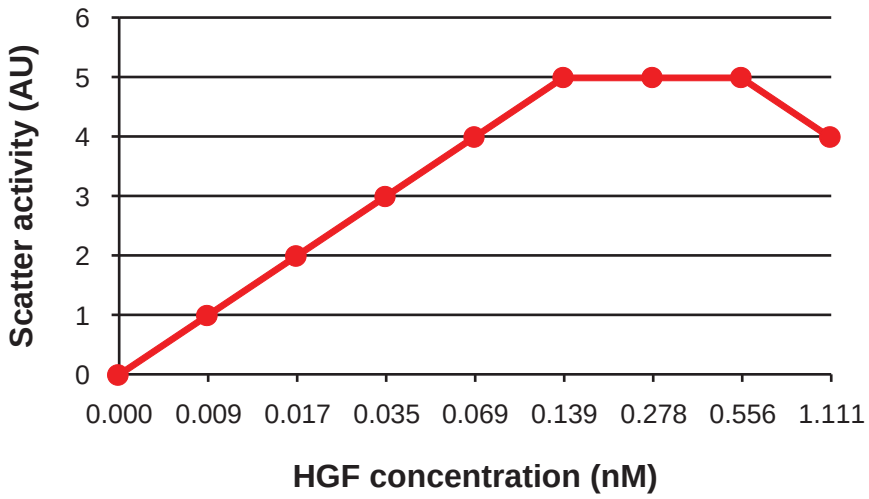

Suppl. Fig. 7. Analysis of HGF-induced scatter activity using HPAF-II human pancreatic adenocarcinoma cells. (A) HPAF-II human pancreatic adenocarcinoma cells were stimulated with the indicated concentrations of HGF and stained with crystal violet 20 hours later. Cell scattering was determined by microscopy. HGF induced dose-dependent cell scattering until it reached saturation at a concentration of 0.14 nM. A scatter activity score was assigned to each HGF concentration within the linear range (0, total absence of cell scattering at 0 ng/ml HGF; 5, maximum cell scattering at 0.14 nM HGF). Magnification: 100X. (B) Graphic representation of HGF-induced scatter activity using HPAF-II cells and the scoring system described in A.

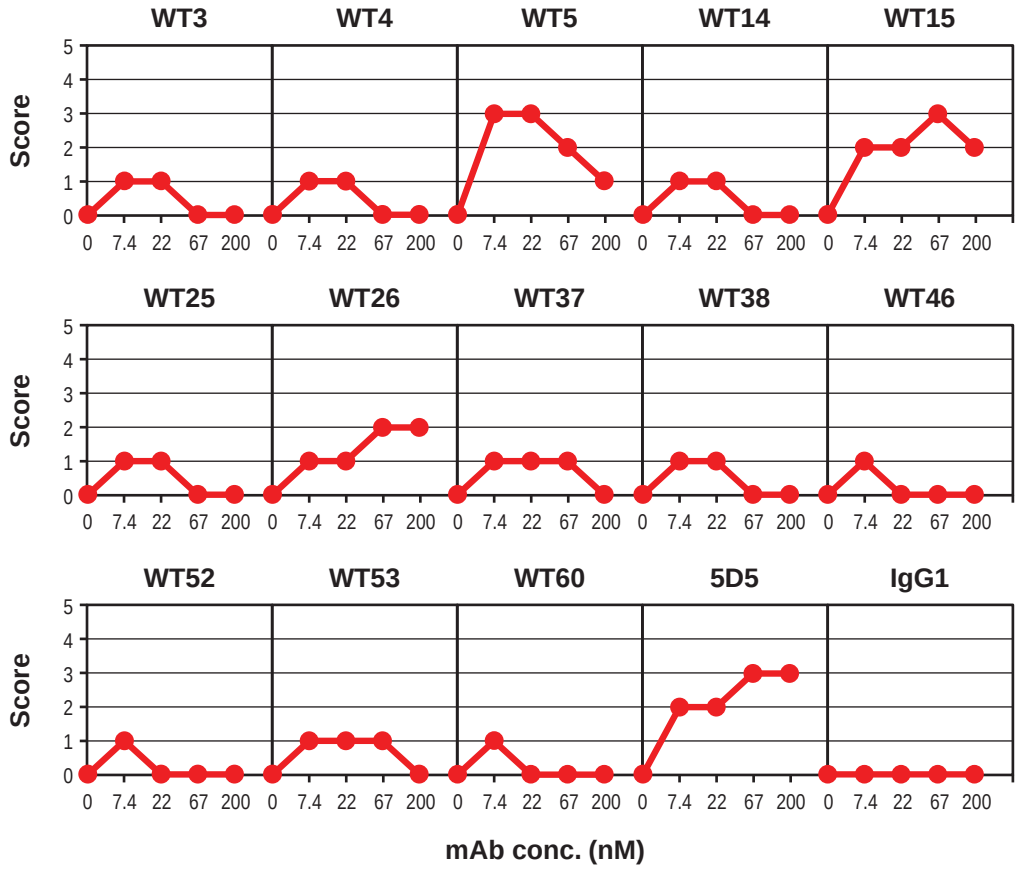

Suppl. Fig. 8. Agonistic activity of anti-Met antibodies as measured by their ability to promote cell scattering. HPAF-II human pancreatic adenocarcinoma cells were incubated with increasing concentrations of antibodies (0, 7.4, 22, 67 and 200 nM) in the absence of HGF. Scatter activity was quantified using a scoring system based on a standard HGF curve ranging from 0 (total absence of cell scattering in the absence of HGF) to 5 (maximum cell scattering in the presence of 0.14 nM HGF; see Suppl. Fig. 7). Values on the X and Y axis represent mAb concentration (nM) and scatter score, respectively. The 5D5 agonistic antibody and an irrelevant IgG1 were used as positive and negative control, respectively.

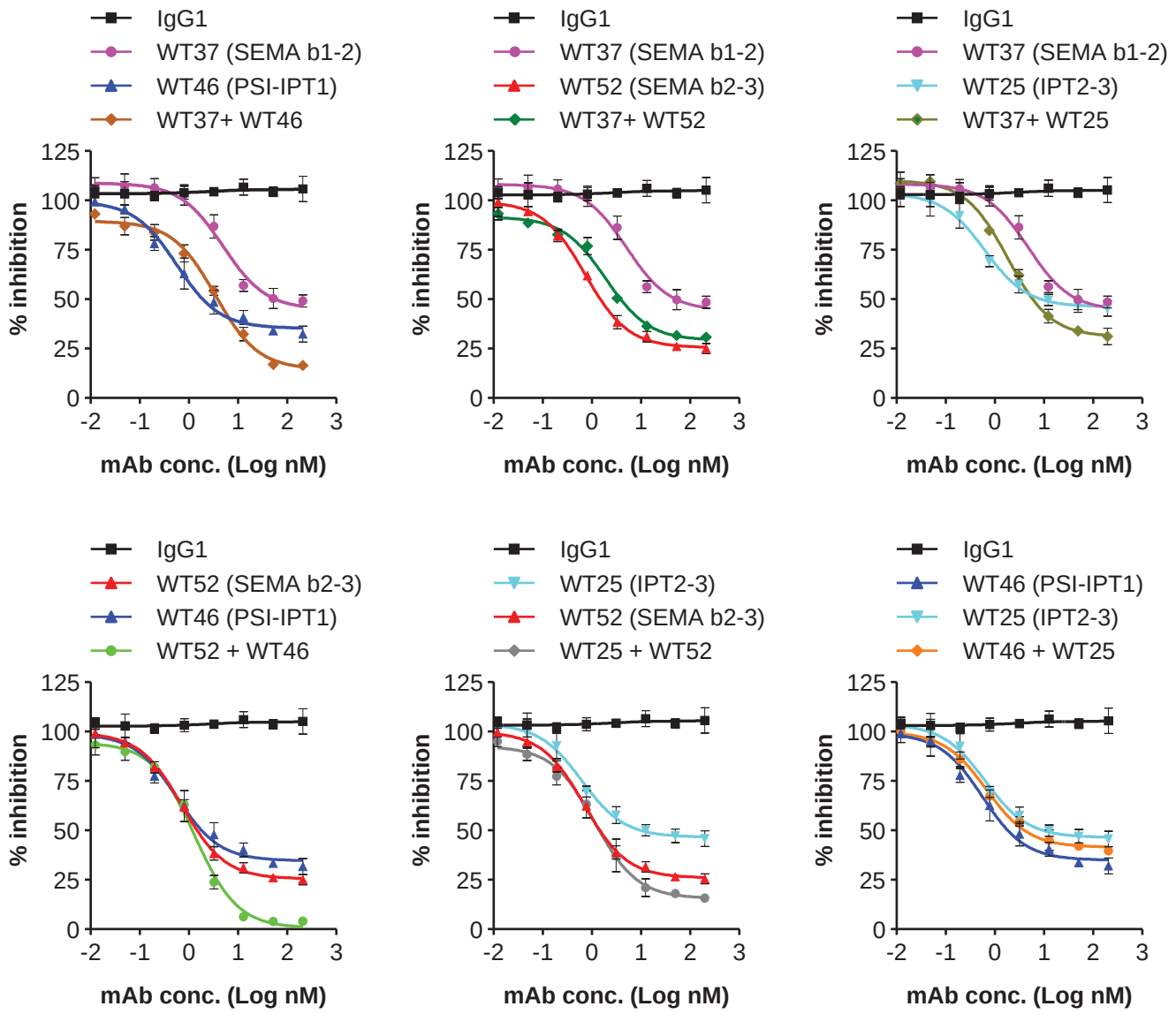

Suppl. Fig. 9. Antagonistic activity of antibody combinations as measured by their ability to inhibit HGF-dependent Met autophosphorylation. A549 human lung carcinoma cells were stimulated with recombinant HGF (1 nM) in the presence of increasing concentrations (0-200 nM) of either single mAbs or a 1:1 combination of two different mAbs (200 nM of either mAb 1 or mAb 2 is compared with 100 nM of mAb 1 + 100 nM of mAb 2, and so on). Met autophosphorylation was determined by ELISA using anti-phospho-Met antibodies. An irrelevant human IgG1 was used as negative control.

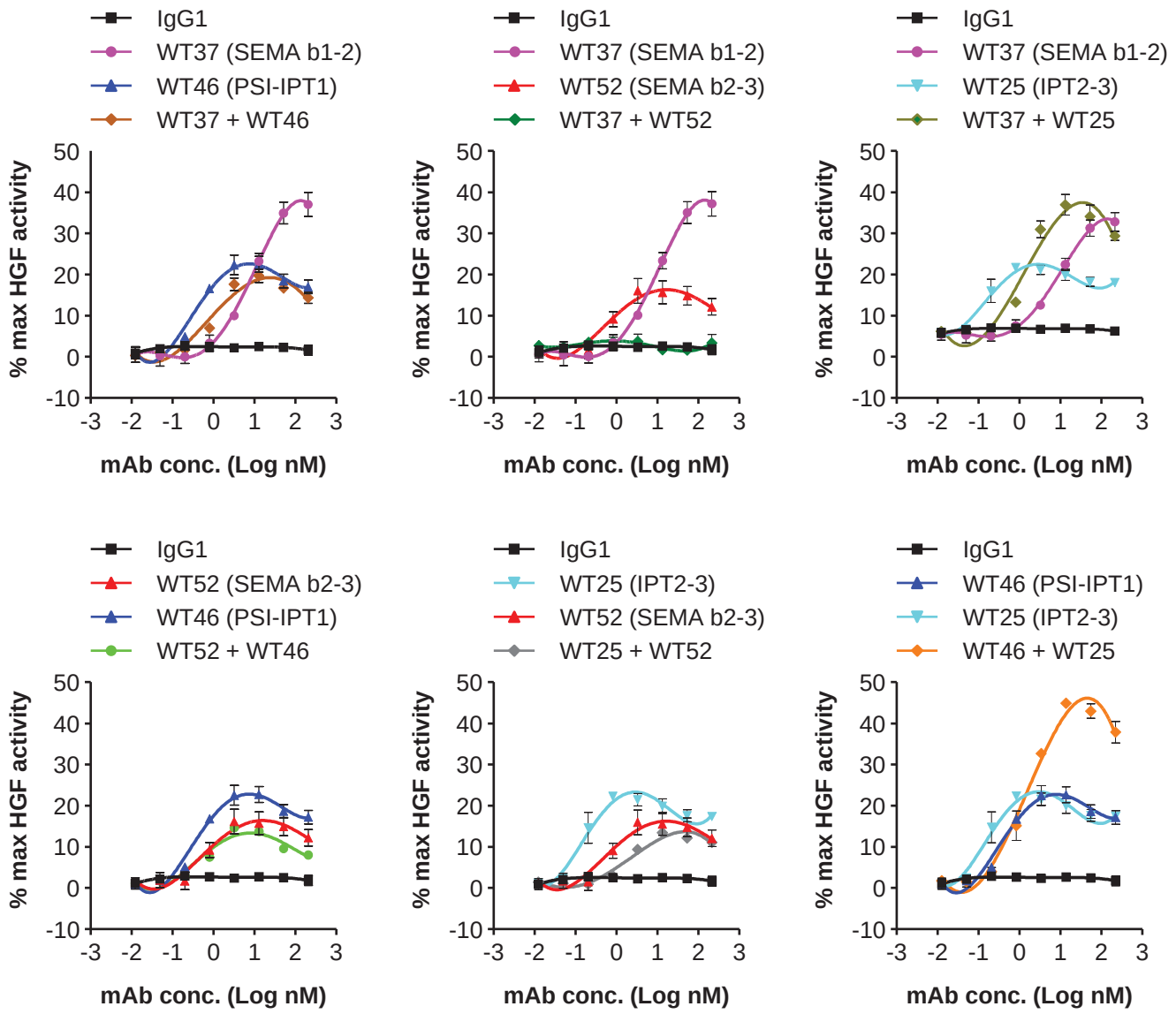

Suppl. Fig. 10. Agonistic activity of antibody combinations as measured by their ability to promote Met autophosphorylation. A549 human lung carcinoma cells were stimulated with increasing concentrations (0-200 nM) of either single mAbs or a 1:1 combination of two different mAbs (200 nM of either mAb 1 or mAb 2 is compared with 100 nM of mAb 1 + 100 nM of mAb 2, and so on). At the same time, cells were also stimulated with increasing concentrations of recombinant HGF as a control. Met autophosphorylation was determined by ELISA using anti-phospho-Met antibodies. The agonistic activity of mAbs was expressed as percent maximal HGF activity. An irrelevant human IgG1 was used as negative control.

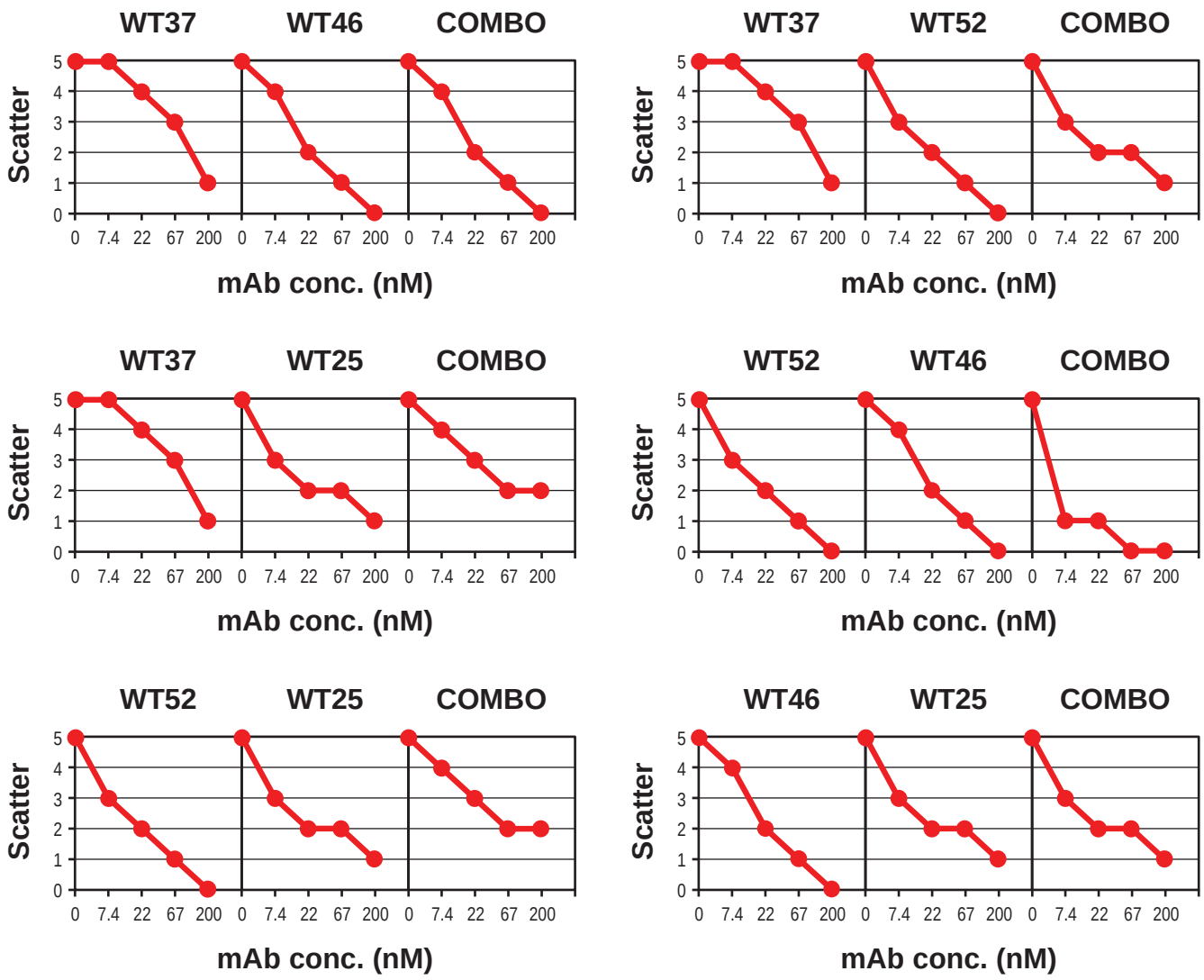

Suppl. Fig. 11. Antagonistic activity of antibody combinations as measured by their ability to inhibit HGF-induced cell scattering. HPAF-II human pancreatic adenocarcinoma cells were incubated with 0.14 nM HGF in the presence of increasing concentrations of either single antibodies (0, 7.4, 22, 67 and 200 nM) or a 1:1 combination of two antibodies (200 nM of mAb 1 and mAb 2 are compared with 100 nM of mAb 1 + 100 nM of mAb 2, and so on). Scatter activity was quantified using a scoring system based on a standard HGF curve ranging from 0 (total absence of cell scattering in the absence of HGF) to 5 (maximum cell scattering in the presence of 0.14 nM HGF; see Suppl. Fig. 7). Values on the X and Y axis represent mAb concentration (nM) and scatter score, respectively.

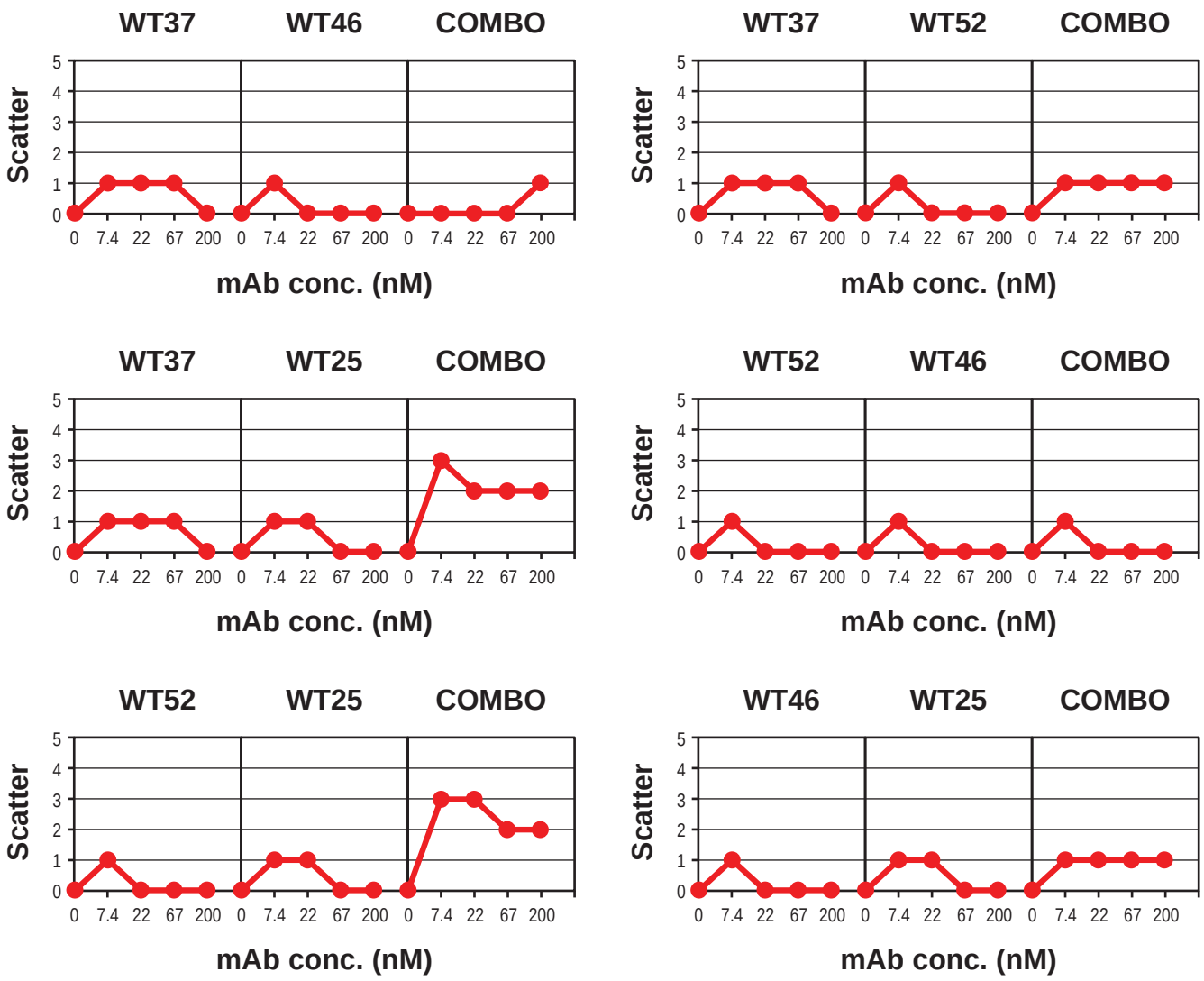

Suppl. Fig. 12. Agonistic activity of antibody combinations as measured by their ability to promote cell scattering. HPAF-II human pancreatic adenocarcinoma cells were incubated with increasing concentrations of either single antibodies (0, 7.4, 22, 67 and 200 nM) or a 1:1 combination of two antibodies (200 nM of mAb 1 and mAb 2 are compared with 100 nM of mAb 1 + 100 nM of mAb 2, and so on). Scatter activity was quantified using a scoring system based on a standard HGF curve ranging from 0 (total absence of cell scattering in the absence of HGF) to 5 (maximum cell scattering in the presence of 0.14 nM HGF; see Suppl. Fig. 7). Values on the X and Y axis represent mAb concentration (nM) and scatter score, respectively.

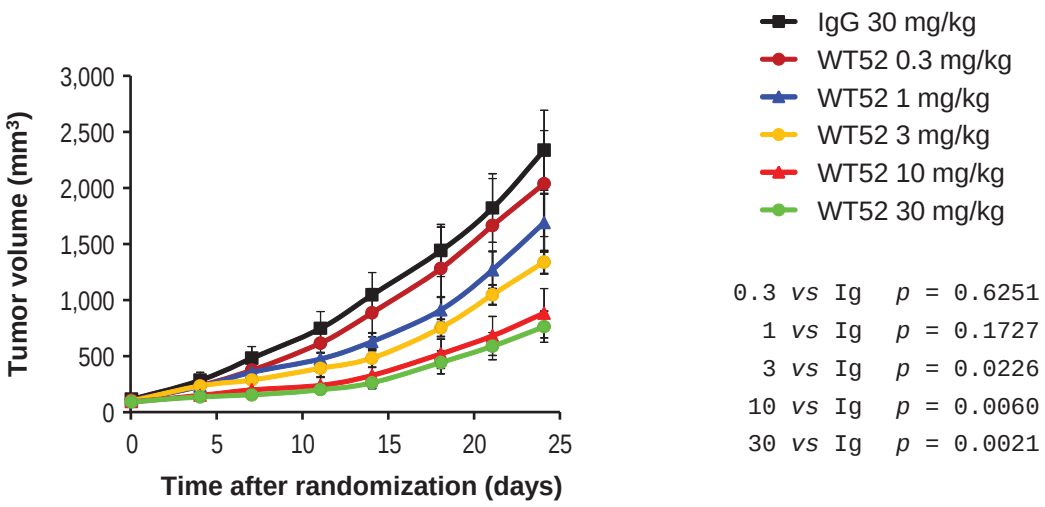

Suppl. Figure 13. Anti-Met antibodies display dose-dependent anti-tumor activity in a human xenograft model. U87-MG human glioma cells, that express both Met and HGF, were injected subcutaneously into NOD-SCID mice. Mice were stratified based on tumor volume and divided into several homogeneous groups (n = 6), which were randomly assigned to the indicated treatment arms. Antibodies were administered twice weekly at the appropriate dose by i.p injection, and tumor growth was followed over time by caliper measurement. Statistical significance was determined by a Student's T-test and is relative to the latest measurement time. The figure shows a representative dose escalation experiment using WT52. Similar results were obtained using WT46. However, as a general trend, WT52 was slightly more effective than WT46 at all doses tested.

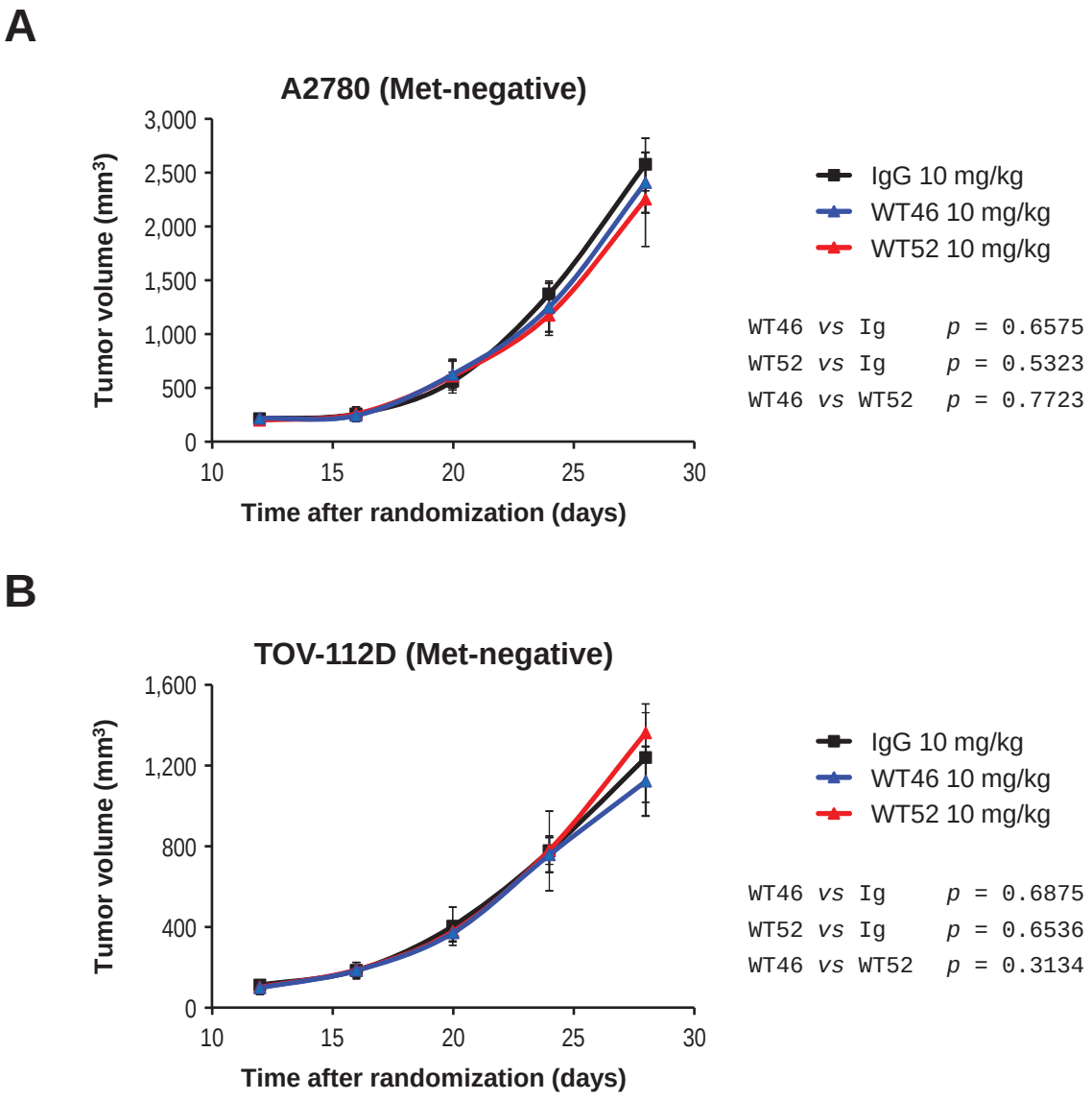

Suppl. Figure 14. Anti-Met antibodies do not display any anti-tumor activity in two Met-negative human xenograft models. In order to assess their specificity, anti-Met antibodies were tested in two human xenograft models not expressing Met at both the protein and mRNA level. A2780 (A) and TOV-112D (B) human ovarian carcinoma cells were injected subcutaneously into NOD-SCID mice. Following randomization, mice were assigned to three treatment arms (irrelevant IgG1, 10 mg/kg; WT52, 10 mg/kg; WT46, 10 mg/kg; *n* = 6). Antibodies were administered twice weekly by i.p injection, and tumor growth was followed over time by caliper measurement. Statistical significance was determined by a Student's T-test and is relative to the latest measurement time.

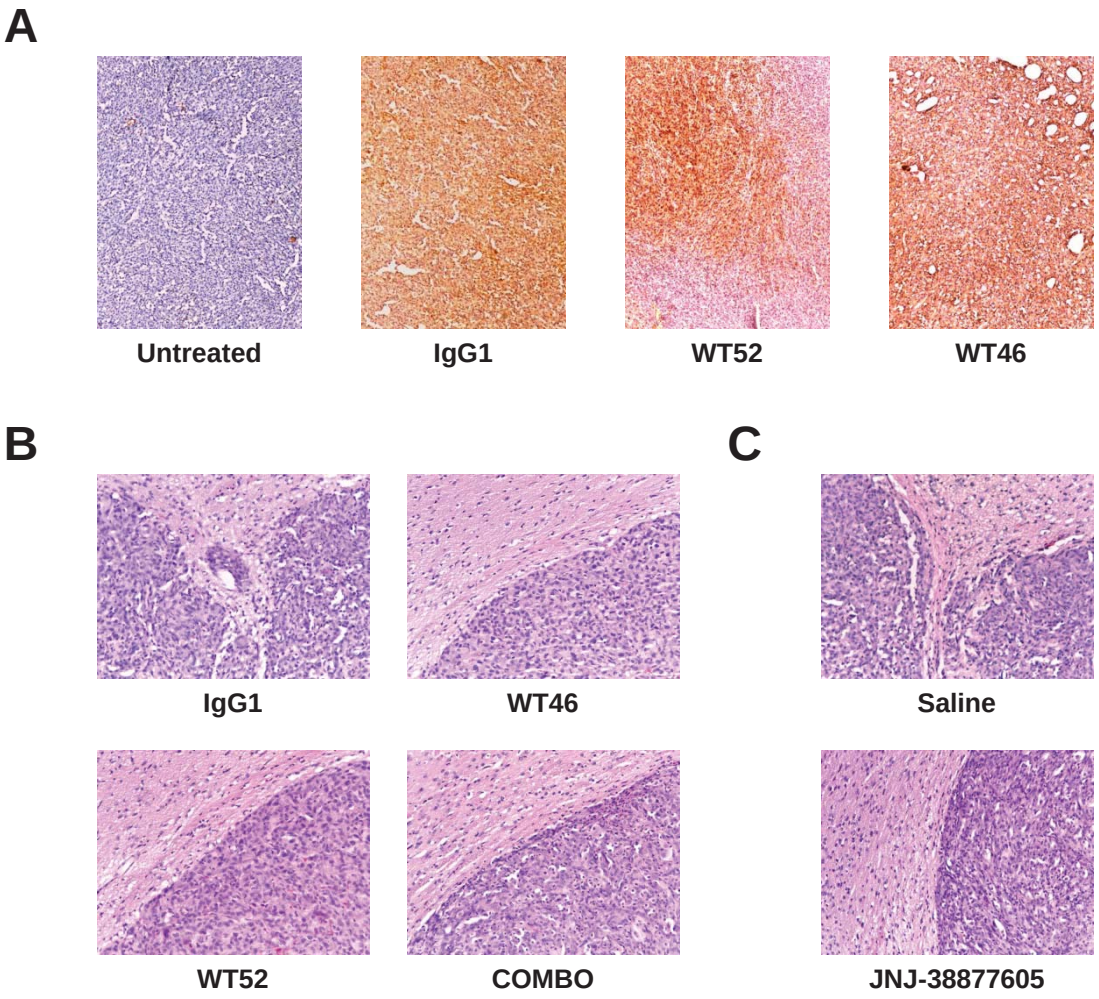

Suppl. Fig. 15. Immunohistochemical and histological analysis of U87-MG orthotopic tumors. (A) CD-1 nude mice bearing orthotopic U87-MG glioma cell experimental tumors were treated with either an irrelevant IgG1 (10 mg/kg), WT52 (10 mg/kg), WT46 (10 mg/kg), or a combination of WT52 and WT46 (5 + 5 mg/kg). Mice were sacrificed when showing manifest neurological symptoms, and brains were extracted for analysis. Tumor-containing brain sections were analyzed by immunohistochemistry using anti-human Fc antibodies. Sections from untreated mice were used as negative controls. Magnification: 100X. (B) Histological analysis of brain sections stained with hematoxylin and eosin showing representative images of tumor-brain interfaces. Magnification: 100X. (C) CD-1 nude mice bearing orthotopic U87-MG tumors were treated either with physiologic solution (saline) or with 20 mg/kg JNJ-38877605. Upon autopsy, brain sections were analyzed by histology as above. Magnification: 100X.

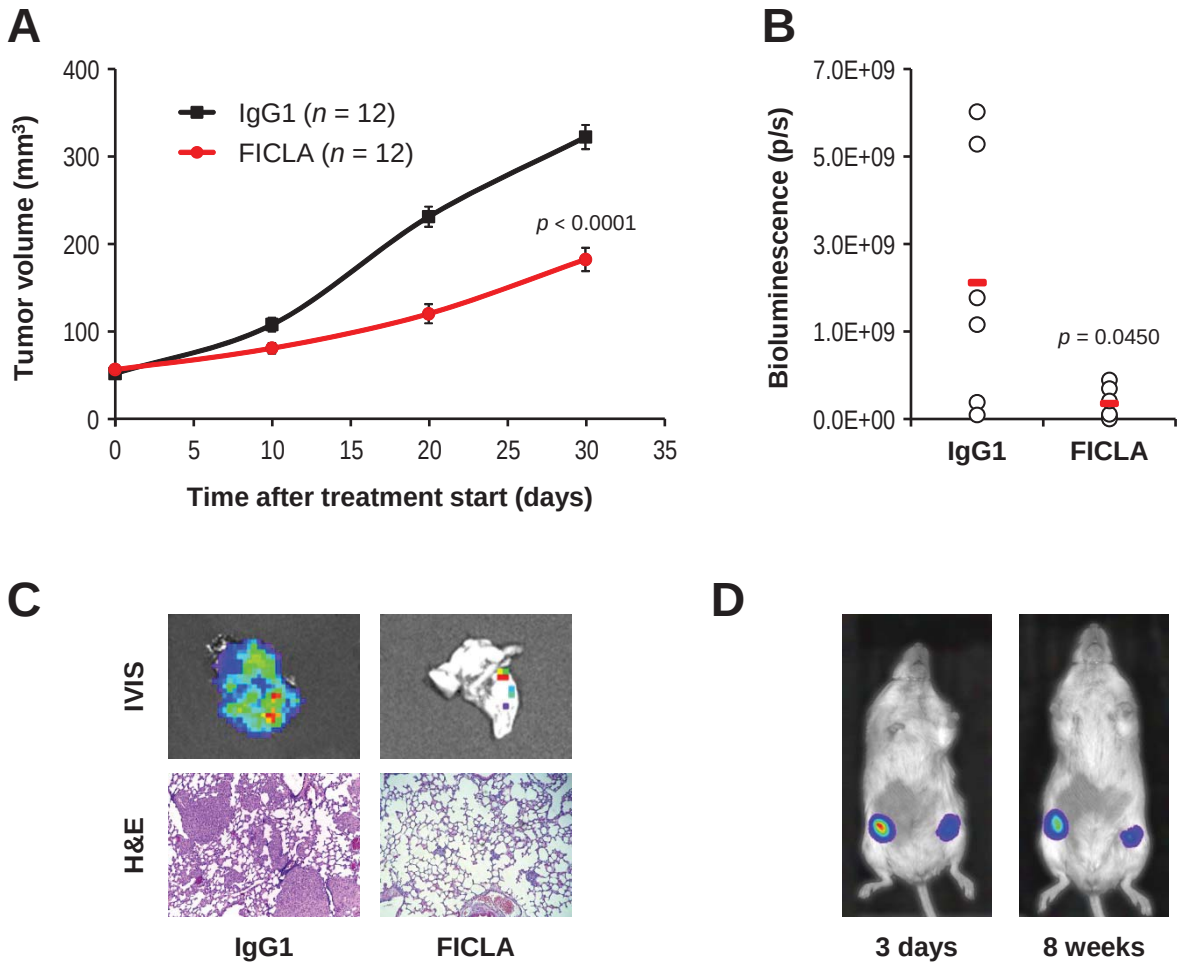

Suppl. Figure 16. Set up of a HGF-dependent orthotopic mouse model of triple-negative mammary carcinoma. Luciferase-expressing MDA-MB-231 human triple-negative mammary carcinoma cells are injected into the mammary fat pad of NOD-SCID mice along with HGF-secreting human mammary fibroblasts. Following randomization, mice are assigned to the desired treatment arms. Tumor growth is followed over time by caliper measurement. After four weeks, neoadjuvant treatment is interrupted and tumors are removed by surgery. Two weeks after, mice are sacrificed and subjected to autopsy. Metastases can be detected by bioluminescence analysis of explanted organs. (A) Inhibition of tumor growth by an anti-human HGF neutralizing antibody (ficlatuzumab; a kind gift of AVEO Pharmaceuticals) provides evidence that this model is HGF-dependent. Statistical significance was calculated by a Student's T-test (n = 12). (B) Bioluminescence analysis demonstrates that ficlatuzumab also inhibits metastatic dissemination to the lung. Statistical significance was determined as in A (n = 6). (C) Histological analysis of lung sections (H&E) confirms that inhibition of HGF/Met reduces pulmonary metastases and validate bioluminescence results (IVIS). (D) A symmetrical experiment conducted using luciferase-expressing human mammary fibroblasts and wild-type MDA-MB-231 cells indicates that implanted fibroblasts persist at the site of injection for several weeks.

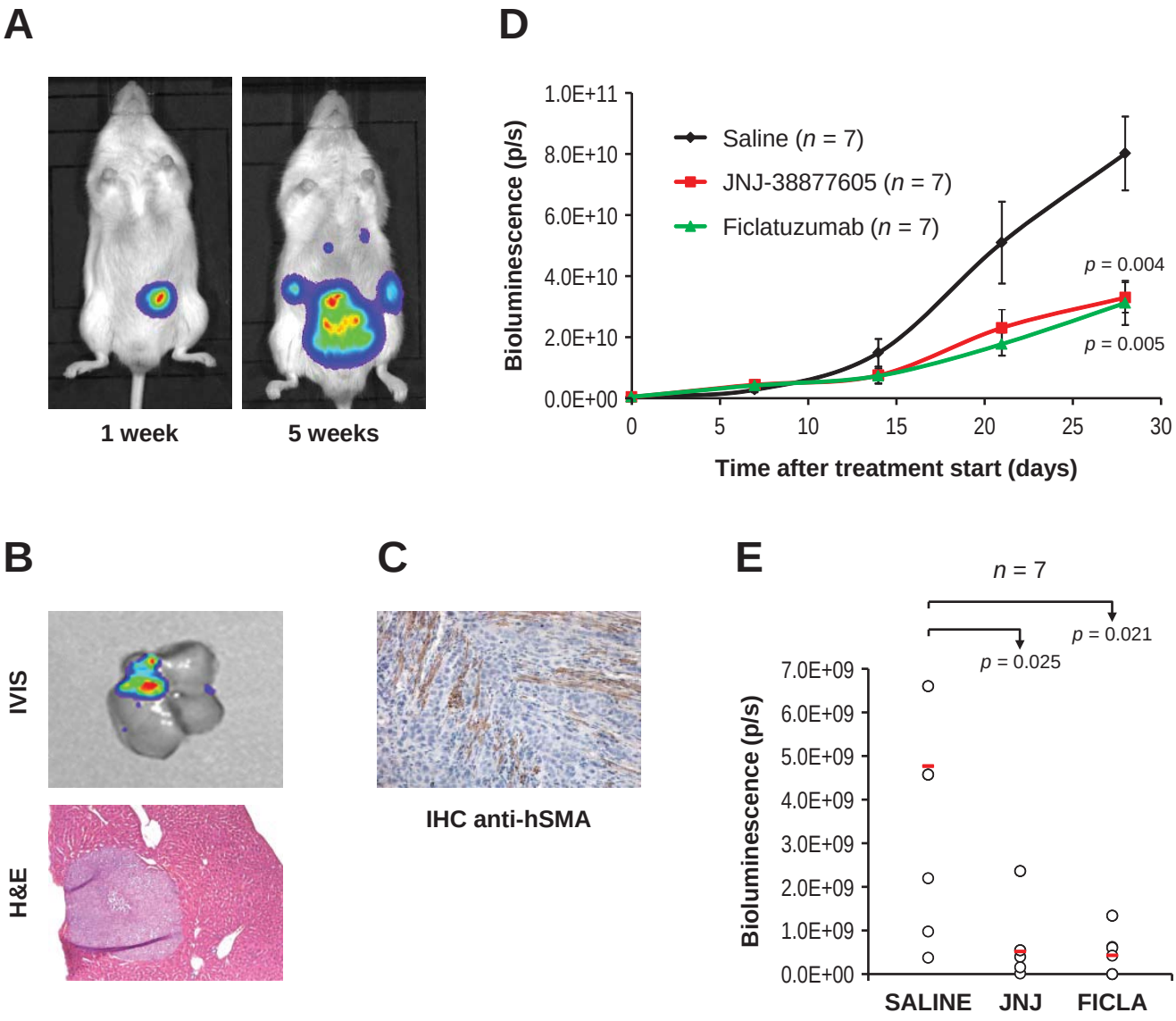

Suppl. Figure 17. Set up of a HGF-dependent orthotopic mouse model of colon carcinoma. Luciferase-expressing HCT-116 human colorectal carcinoma cells are microinjected into the cecum submucosa of NOD-SCID mice along with HGF-secreting human colon myofibroblasts. (A) Tumor growth over time can be assessed by whole body bioluminescence. (B) Metastatic dissemination can be determined by bioluminescence analysis (IVIS) of explanted organs, which gives results consistent with conventional histology (H&E). (C) Immunohistochemical analysis of tumor sections using human-specific anti-smooth muscle actin antibodies demonstrates persistence of human myofibroblasts. (D) Tumor growth in this model is HGF-dependent, as it can be inhibited by either a small molecule Met inhibitor (JNJ-38877605) or an anti-human HGF neutralizing antibody (ficlatuzumab). Statistical significance relative to control (saline) was calculated by a Student's T-test (n = 7). (E) Metastatic spreading to the liver is HGF-dependent as it can be prevented by the same treatments described in D. The red bar indicates the mean. Statistical significance was calculated as in D.

Clone	Library	Llama #	VH family
WT1	λ1	1	2
WT2	κ1	1	26
WT3	λ2	2	14
WT4	λ2	2	15
WT5	λ2	2	16
WT6	λ2	2	19
WT7	λ2	2	21
WT8	λ2	2	25
WT9	λ2	2	24
WT10	κ2	2	3
WT11	κ2	2	4
WT12	κ2	2	20
WT13	κ3	3	1
WT14	λ3	3	6
WT15	λ3	3	6
WT16	λ3	3	6
WT17	λ3	3	6
WT18	λ3	3	6
WT19	λ3	3	6
WT20	λ3	3	6
WT21	κ3	3	9
WT22	κ3	3	10
WT23	λ3	3	18
WT24	κ3	3	23
WT25	λ4	4	7
WT26	λ4	4	8
WT27	λ4	4	8
WT28	λ4	4	8
WT29	λ4	4	12
WT30	λ4	4	13
WT31	λ4	4	17
WT32	λ4	4	22
WT33	κ4	4	5

Clone	Library	Llama #	VH family
WT34	λ5	5	30
WT35	λ5	5	31
WT36	λ5	5	32
WT37	λ5	5	33
WT38	κ5	5	28
WT39	κ5	5	28
WT40	κ5	5	28
WT41	κ5	5	28
WT42	κ5	5	28
WT43	κ5	5	28
WT44	κ5	5	28
WT45	κ5	5	28
WT46	κ5	5	28
WT47	κ5	5	28
WT48	κ5	5	28
WT49	κ5	5	28
WT50	λ7	6	29
WT51	λ7	6	29
WT52	λ7	6	29
WT53	λ7	6	29
WT54	κ7	6	27
WT55	κ7	6	27
WT56	κ7	6	27
WT57	κ7	6	27
WT58	κ7	6	27
WT59	κ7	6	27
WT60	κ7	6	27
WT61	κ7	6	27
WT62	κ7	6	27
WT63	κ7	6	27
WT64	κ7	6	27
WT65	κ7	6	27
WT66	κ7	6	27
WT67	κ7	6	27
WT68	κ7	6	27

Suppl. Tab. 1. Fab clones that inhibit HGF binding to Met in ELISA. Clones that scored positive in the ELISA-based screening described in Suppl. Fig. 2 were sequenced in the VH and VL regions and divided into families based on their VH CDR3 sequence. This procedure identified 68 HGF-competing Fabs (WT1-68) belonging to 32 different VH families. The table shows the clone name, the library from which it was identified (λ or κ), the llama from which the library was derived (color coded), and the corresponding VH family number. Family number was assigned arbitrarily and does not reflect IMTG (International Immunogenetics Information System) nomenclature.

ANTIBODY		RECEPTOR BINDING ACTIVITY						
Clone	llama #	human Met	mouse Met	llama Met	MSPR	EGFR	PDGFR	VEGFR
WT3	2	+	–	–	–	–	–	–
WT4	2	+	–	–	–	–	–	–
WT5	2	+	–	–	–	–	–	–
WT14	3	+	–	–	–	–	–	–
WT15	3	+	–	–	–	–	–	–
WT25	4	+	–	–	–	–	–	–
WT26	4	+	–	–	–	–	–	–
WT37	5	+	–	–	–	–	–	–
WT38	5	+	–	–	–	–	–	–
WT46	5	+	–	–	–	–	–	–
WT52	6	+	–	–	–	–	–	–
WT53	6	+	–	–	–	–	–	–
WT60	6	+	–	–	–	–	–	–
224G11	N/A	+	–	–	–	–	–	–
5D5	N/A	+	–	–	–	–	–	–
CTX	N/A	–	–	–	–	+	–	–
IgG1	N/A	–	–	–	–	–	–	–
hrHGF	N/A	+	+	+	–	–	–	–

Suppl. Tab. 2. Anti-Met antibodies bind specifically to human Met. The specificity of anti-Met antibodies was tested by ELISA using a series of recombinant proteins corresponding to the extracellular portions of a variety of receptor tyrosine kinases. Recombinant receptors were immobilized in solid phase and incubated with increasing concentrations of the indicated antibodies in solution. Binding was revealed using horseradish peroxidase-conjugated anti-human Fc secondary antibodies. Control antibodies included two anti-Met antibodies (224G11, 5D5), cetuximab (CTX) and an irrelevant human IgG1. Binding of recombinant human HGF (rhHGF) was also tested to the same receptors using biotinylated anti-HGF antibodies and horseradish peroxidase-conjugated strepdavidin. MSPR, Macrophage Stimulating Protein Receptor; EGFR, Epidermal Growth Factor Receptor; PDGFR, Platelet Derived Growth Factor Receptor; VEGFR, Vascular Endothelial Growth Factor Receptor; N/A, not applicable.

mAb	HM	LM	LS1	LS2	LS3	LS4	LS5	LP6	LP7	LI8	LI9	LI10	LI11	LI12	LI13	LI14	binding domain
WT3	+	−	+	−	−	−	−	n.t.	n.t.	n.t.	n.t.	n.t.	n.t.	n.t.	n.t.	n.t.	blades 2-3
WT5	+	−	+	+	+	−	−	n.t.	n.t.	n.t.	n.t.	n.t.	n.t.	n.t.	n.t.	n.t.	blade 5
WT37	+	−	−	−	−	−	−	n.t.	n.t.	n.t.	n.t.	n.t.	n.t.	n.t.	n.t.	n.t.	blades 1-2
WT52	+	−	+	−	−	−	−	n.t.	n.t.	n.t.	n.t.	n.t.	n.t.	n.t.	n.t.	n.t.	blades 2-3
WT53	+	−	+	−	−	−	−	n.t.	n.t.	n.t.	n.t.	n.t.	n.t.	n.t.	n.t.	n.t.	blades 2-3
WT14	+	−	n.t.	n.t.	n.t.	n.t.	n.t.	−	−	+/−	+/−	+/−	+	+	+	+	PSI-IPT 1
WT15	+	−	n.t.	n.t.	n.t.	n.t.	n.t.	−	−	+/−	+/−	+/−	+	+	+	+	PSI-IPT 1
WT38	+	−	n.t.	n.t.	n.t.	n.t.	n.t.	−	−	+/−	+/−	+/−	+	+	+	+	PSI-IPT 1
WT46	+	−	n.t.	n.t.	n.t.	n.t.	n.t.	−	−	+/−	+/−	+/−	+	+	+	+	PSI-IPT 1
WT60	+	−	n.t.	n.t.	n.t.	n.t.	n.t.	−	−	+/−	+/−	+/−	+	+	+	+	PSI-IPT 1
WT4	+	−	n.t.	n.t.	n.t.	n.t.	n.t.	−	−	−	−	−	−	−	+/−	+	IPT 2-3
WT25	+	−	n.t.	n.t.	n.t.	n.t.	n.t.	−	−	−	−	−	−	−	+/−	+	IPT 2-3
WT26	+	−	n.t.	n.t.	n.t.	n.t.	n.t.	−	−	−	−	−	−	−	+/−	+	IPT 2-3
5D5	+	−	+	+	+	−	−	n.t.	n.t.	n.t.	n.t.	n.t.	n.t.	n.t.	n.t.	n.t.	blade 5
224G11	+	−	n.t.	n.t.	n.t.	n.t.	n.t.	−	−	−	+/−	+	+	+	+	+	IPT 1

Suppl. Tab. 3. Mapping of the epitopes recognized by HGF-displacing anti-Met antibodies. The results obtained with Met deletion mutants suggest that HGF-displacing anti-human Met antibodies bind to both the SEMA and IPT region of Met (Suppl. Fig. 4B). To more finely map the epitopes recognized by these mAbs, we analyzed their ability to bind to llama-human chimeras spanning the entire extra-cellular domain of Met (Suppl. Fig. 5). This analysis reveled that three of the five SEMA-binding antibodies (WT3, WT52, WT53) recognize an epitope located within blades 2 and 3. The other two SEMA-binding antibodies (WT5, WT37) recognize epitopes located within blade 5 and blades 1-2, respectively. All antibodies binding to SEMA-PSI-IPT 1-2 but not to SEMA-PSI (WT14, WT15, WT38, WT46, WT60) recognize an epitope located across the PSI domain and IPT domain 1. The three antibodies binding to Decoy Met only (WT4, WT25, WT26) recognize an epitope located across IPT domains 2 and 3. Finally, the 5D5 and 224G11 control antibodies bind to blade 5 and IPT 1, respectively. Color code is the same as in Suppl. Fig. 4. HM, human Met; LM, llama Met; n.t., not tested.

HGF-COMPETING ANTIBODY		COMPETES WITH:	
Clone	Binding domain	5D5	224G11
WT3	blades 2-3	NO	NO
WT4	IPT 2-3	NO	NO
WT5	blade 5	YES	YES
WT14	PSI-IPT 1	YES	YES
WT15	PSI-IPT 1	YES	YES
WT25	IPT 2-3	NO	NO
WT26	IPT 2-3	NO	NO
WT37	blades 1-2	NO	NO
WT38	PSI-IPT 1	YES	YES
WT46	PSI-IPT 1	YES	YES
WT52	blades 2-3	NO	NO
WT53	blades 2-3	NO	NO
WT60	PSI-IPT 1	YES	YES
5D5	Blade 5	-	YES
224G11	IPT 1	YES	-

Suppl. Tab. 4. Antibodies directed against the fifth blade of the SEMA domain compete for binding to Met with antibodies directed against the PSI-IPT 1 domains. Competition between antibodies was analyzed by ELISA using biotinylated 5D5 and 224G11 (which bind to SEMA blade 5 and IPT 1, respectively). Briefly, a Met-Fc protein was adsorbed in solid phase and incubated with a fixed concentration of either biotin-5D5 or biotin-224G11 in the presence of increasing concentrations of the indicated antibodies (left column). Binding was revealed using streptavidin conjugated with horseradish peroxidase. Identical results were obtained using Fabs instead of mAbs.

SUPPLEMENTARY METHODS

Cell culture

MKN-45 human gastric carcinoma cells were purchased from the Deutsche Sammlung von Mikroorganismen und Zellkulturen (DSMZ). A549 human lung carcinoma cells, HPAF-II human pancreatic adenocarcinoma cells, U87-MG human glioblastoma cells, TOV-112D and A2780 ovarian carcinoma cells, MDA-MB-231 human mammary adenocarcinoma cells and HCT-116 colorectal carcinoma cells were obtained from the European Collection of Cell Cultures and cultured as suggested by the supplier. Immortalized human mammary fibroblasts (1) are a gift of Bob Weinberg (Whitehead Institute for Biomedical Research, Cambridge, Massachusetts). Human primary colon myofibroblasts, obtained from the European Collection of Cell Cultures, were immortalized using a human TERT lentiviral vector (courtesy of Francesco Galimi, University of Sassari Medical School, Sassari, Italy). The presence of human HGF in mammary and colon fibroblast conditioned medium was analyzed by Western blot using anti-human HGF antibodies (R&D Systems). U87-MG glioma cells, HCT-116 colorectal carcinoma cells and immortalized human mammary fibroblasts cells were engineered to express firefly luciferase by lentiviral vector technology as described (2).

Met autophosphorylation assays

The ability of chimeric mAbs to antagonize HGF-induced Met autophosphorylation was analyzed using A549 human lung carcinoma cells. Serum-starved cells were pre-incubated for

15 minutes with increasing concentrations (0-200 nM) of mAbs and then stimulated with 1 nM recombinant human HGF (R&D Systems) for 15 minutes. Cell lysates were transferred to an ELISA plate pre-coated with anti-human Met antibodies (R&D Systems) and incubated overnight at 4°C. Met auotophosphorylation was determined by ELISA using rabbit anti-phospho-Met antibodies (Y_{1234}-Y_{1235}; Cell Signaling Technology) and revealed using HRP-conjugated anti-rabbit antibodies (Thermo Scientific). The ability of chimeric mAbs to promote Met autophosphorylation in the absence of HGF was also analyzed using A549 cells. Serum-starved cells were incubated for 15 minutes with increasing concentrations (0-200 nM) of mAbs. Met autophosphorylation was determined as described above. In antibody combination experiments, increasing concentrations (0-200 nM) of single mAbs were compared to equal concentrations of a 1:1 mixture of two different mAbs (i.e. 200 nM of either mAb 1 or mAb 2 was compared with 100 nM of mAb 1 + 100 nM of mAb 2 and so on). Met autophosphorylation was determined as described above.

Biological assays

Cell scattering was analyzed using HPAF-II human pancreatic carcinoma cells and quantified using a recombinant human HGF standard curve. Cells were seeded in 96-well plates (7,000 cells/well) and then stimulated with increasing concentrations (0-1.111 nM) of HGF (R&D Systems). After 24 hours, cells were fixed with 11% glutaraldehyde and stained with crystal violet (both from Sigma-Aldrich). Cell scattering was analyzed by microscopy. This analysis revealed that HGF-induced cell scattering reached saturation at 0.139 nM (Suppl. Fig. 7). Based on these results, a scatter score was attributed to cells corresponding to each HGF

concentration ranging from 0 nM to 0.14 nM (0 nM HGF, score = 0; 0.009 nM HGF, score = 1; 0.017 nM HGF, score = 2; 0.035 nM HGF, score = 3; 0.069 nM HGF, score = 4; 0.139 nM HGF, score = 5). To determine the ability of chimeric mAbs to inhibit HGF-induced cell scattering, HPAF-II cells were stimulated with 0.14 nM HGF in the presence of increasing concentrations (0-200 nM) of antibodies. Scatter activity was determined by microscopy using the scoring system described above. The ability of chimeric mAbs to promote HGF-independent cell scattering was analyzed by stimulating HPAF-II cells with increasing concentrations (0-200 nM) of antibodies in the absence of HGF. Scatter activity was determined as above. In antibody combination experiments, single mAbs were compared to mAb mixtures as described for Met autophosphorylation assays. For real-time cell motility assay, HPAF-II cells were seeded in E-plates (7,000 cells/well; Roche Diagnostics), pre-incubated with 200 nM WT52, 200 nM WT46 or 100 nM WT52 + 100 nM WT46, and then stimulated with 0.14 nM HGF. Electrical impedance was monitored continuously for 24 hours, with data recording every fifteen minutes, using a X-celligence RTCA device (Roche Diagnostics). Values were expressed as cell index normalized at the instant of mAb addition. For anchorage-independent cell growth assays, A549 cells were seeded in soft agar in the presence of 0.333 nM HGF and treated twice weekly with 200 nM WT52, 200 nM WT46, or 100 nM WT52 + 100 nM WT46. An irrelevant IgG1 was used as negative control. After three weeks, cell colonies were stained with tetrazolium salts (Sigma-Aldrich), photographed, and quantified using Metamorph software (Molecular Devices).

Subcutaneous xenograft models

U87-MG human glioma cells (4×10^6 cells/mouse) were injected subcutaneously into the

right posterior flank of 7-week old NOD-SCID female mice (Charles River). Tumor growth was monitored over time using a caliper and the formula $V = 4/3\pi\times(1/2x)\times(1/2y)\times(1/2z)$, where *x*, *y* and *z* are the three dimensions of the tumor. Approximately four weeks after cell injection, mice were stratified based on tumor volume (on average measuring between 80 mm^3 and 150 mm^3) and divided into four homogeneous groups ($n = 5$), which were randomly assigned to the following treatment arms: irrelevant IgG1 (10 mg/kg); WT52 (10 mg/kg); WT46 (10 mg/kg); WT52 + WT46 (5 + 5 mg/kg). Antibodies were administered twice weekly by i.p. injection, and mice were sacrificed when tumor volume reached 2,000 mm^3. After five weeks of treatment, the experiment was stopped and all remaining mice sacrificed. For the Met-negative models, NOD-SCID mice were injected subcutaneously with A2780 (3) or TOV-112D (4) human ovarian carcinoma cells (6×10^6 and 5×10^6 cells/mouse, respectively). Tumor-bearing animals were randomized and assigned to three treatment arms (irrelevant IgG1, 10 mg/ml; WT52, 10 mg/ml; WT46, 10 mg/ml; $n = 6$). Antibodies were administered twice weekly by i.p injection, and tumor volume was calculated as above.

Glioblastoma model

For the orthotopic glioblastoma model, luciferase-expressing U87-MG human glioma cells (5×10^5 cells/mouse in 5 µl of medium) were micro-injected into the nucleus caudatus/putamen of CD-1 nude mice (Charles River) using a stereotaxic apparatus (Stoelting). After ten days, mice were injected i.p. with D-luciferin (150 mg/kg; Perkin Elmer), stratified based on *in vivo* bioluminescence signal using an IVIS Lumina II apparatus (Perkin Elmer), and randomly assigned to four treatment arms ($n = 6$) as described for the subcutaneous model. Antibodies were

administered twice weekly by i.p. injection with the same dosage described above. Tumor growth over time was assessed by IVIS imaging. Mice were sacrificed when showing manifest neurological symptoms, and the experiment was stopped after eight weeks of treatment. Prior to sacrifice, mice were perfused with 4% paraformaldehyde (Sigma-Aldrich), and brains were embedded in paraffin. Brain sections containing the tumor were analyzed by immunohistochemistry using biotinylated anti-human Fc antibodies (Abnova). Staining was revealed with HRP-conjugated streptavidin (Sigma-Aldrich). Histology was analyzed on sections stained with hematoxylin and eosin (Bio-Optica).

Orthotopic mammary carcinoma model

Luciferase-expressing MDA-MB-231 human triple-negative mammary carcinoma cells (5×10^5 cells/injection site) were injected bilaterally into the mammary fat pad of immunodeficient NOD-SCID mice (2.5×10^5 cells/injection site) along with immortalized human mammary fibroblasts (1). Tumor growth was monitored over time using a caliper and the formula described above. After two weeks, mice were stratified based on tumor volume and randomly assigned to the following five treatment arms (n = 6): IgG1, 10 mg/kg; WT52, 10 mg/kg; WT46, 10 mg/kg; WT52 + WT46, 5 + 5 mg/kg; JNJ-38877605, 20 mg/kg. Antibodies were administered twice weekly by i.p. injection; JNJ-38877605 (Janssen Research & Development; refs. 5) was administered daily by oral gavage. After four weeks of treatment, tumors were surgically removed, and neoadjuvant therapy was interrupted. Two weeks after surgery, mice were injected with luciferin (Perkin Elmer), sacrificed, and subjected to autopsy. Metastatic dissemination was determined by bioluminescence analysis of isolated lungs. Following

bioluminescence analysis, lungs were embedded in paraffin and processed for histology. Lung sections were stained with hematoxylin and eosin (Bio-Optica) and analyzed by microscopy for the presence of metastases.

Orthotopic colon carcinoma model

Luciferase-expressing, *KRAS*-mutant HCT-116 human colorectal carcinoma cells were micro-injected (1.5×10^6 cells/mouse) into the cecum submucosa of 7 week-old NOD-SCID male mice using a glass microcapillary (6) along with immortalized human colon myofibroblasts (0.5×10^6 cells/mouse). One week after cell injection, mice were stratified into four homogeneous groups based on in vivo bioluminescence signal and randomly assigned to four treatment arms (n = 7) as above (IgG1, 10 mg/kg; WT52, 10 mg/kg; WT46, 10 mg/kg; WT52 + WT46, 5 + 5 mg/kg). Antibodies were administered twice weekly by i.p. injection. After four weeks of treatment, mice were injected with luciferin (Perkin Elmer), sacrificed, and their livers extracted for bioluminescence assessment. Following IVIS imaging, organs were embedded in paraffin and processed for histological analysis. Liver sections stained with hematoxylin and eosin were analyzed for the presence of metastases. The persistence of human myofibroblasts was analyzed by immunohistochemistry using human-specific anti-smooth muscle actin antibodies (Abcam).

REFERENCES

1. Kuperwasser C, Chavarria T, Wu M, Magrane G, Gray JW, Carey L, Richardson A, Weinberg RA. Reconstruction of functionally normal and malignant human breast tissues in mice. *Proc Natl Acad Sci USA.* 2004; 101(14):4966-4971.

2. Follenzi A, Naldini L. Generation of HIV-1 derived lentiviral vectors. *Methods Enzymol.* 2002; 346:454-465.

3. Maggiora P, Lorenzato A, Fracchioli S, Costa B, Castagnaro M, Arisio R, Katsaros D, Massobrio M, Comoglio PM, Flavia Di Renzo M. The RON and MET oncogenes are co-expressed in human ovarian carcinomas and cooperate in activating invasiveness. *Exp Cell Res.* 2003; 288(2):382-389.

4. Michieli P, Mazzone M, Basilico C, Cavassa S, Sottile A, Naldini L, Comoglio PM. Targeting the tumor and its microenvironment by a dual-function decoy Met receptor. *Cancer Cell.* 2004; 6(1):61-73.

5. Galimi F, Torti D, Sassi F, Isella C, Corà D, Gastaldi S, Ribero D, Muratore A, Massucco P, Siatis D, Paraluppi G, Gonella F, Maione F, Pisacane A, David E, Torchio B, Risio M, Salizzoni M, Capussotti L, Perera T, Medico E, Di Renzo MF, Comoglio PM, Trusolino L, Bertotti A. Genetic and expression analysis of MET, MACC1, and HGF in metastatic colorectal cancer: response to MET inhibition in patient xenografts and pathologic correlations. *Clin Cancer Res.* 2011; 17(10):3146-3156.

6. Céspedes MV, Espina C, García-Cabezas MA, Trias M, Boluda A, Gómez del Pulgar MT, Sancho FJ, Nistal M, Lacal JC, Mangues R. Orthotopic microinjection of human colon cancer cells in nude mice induces tumor foci in all clinically relevant metastatic sites. *Am J Pathol.* 2007; 170(3):1077-1085.